Clays and Clay Minerals, Vol. 50, No. 6, 771–783, 2002.

EFFECT OF ACID AND ALKALI TREATMENTS ON SURFACE AREAS AND ADSORPTION ENERGIES OF SELECTED MINERALS

GRZEGORZ JOZEFACIUK* AND GRZEGORZ BOWANKO

Institute of Agrophysics of Polish Academy of Sciences, Doswiadczalna 4 str., 20-290 Lublin, Poland

Abstract—Bentonite, biotite, illite, kaolin, vermiculite and zeolite were acidified or alkalized with hydrochloric acid or sodium hydroxide at concentrations of 0.1, 1.0 and 5.0 mole dm^{-3} at room temperature for two weeks. In acid treatments, dissolution of Al prevailed over Si and the opposite was observed in alkali treatments. The XRD patterns showed severe alteration of the crystal structure after acid treatments, whereas sharpening of the XRD peaks after alkali treatments was observed. Illite and kaolin were most resistant to acid attack. With a few exceptions, the surface areas of the minerals computed from both water and nitrogen adsorption isotherms increased with acid and alkali treatments. With increasing reagent concentration, the nitrogen surface area increased faster than the water surface area. Well-defined trends were not noted in either changes of average water or nitrogen adsorption energies or in relative amounts of adsorption sites, indicating that the effects of acid and alkali attack are controlled by the individual character of the minerals.

Key Words—Acidification, Adsorption Energy, Alkalization, Nitrogen Adsorption, Surface Area, Water Vapor Adsorption.

INTRODUCTION

Acid and alkali effects are important controls over mineral weathering (Frank and Gebhardt, 1991; Jackson and Sherman, 1952, 1989; Yatsu, 1988) and genesis (Chermak and Rimstidt, 1987; Drief *et al.*, 2001; Eberl *et al.*, 1993; Huang, 1993). Treatment of minerals with inorganic acids of rather high concentrations and usually at elevated temperatures, referred to as 'acid activation', is commonly used for production of sorbents or catalysts (white carbon blacks) used in industry or environmental protection measures (Bandosz *et al.*, 1992; Bergaya and Lagaly, 2001; Breen *et al.*, 1995; Brown and Rhodes, 1995; Ravichandran and Sivasankar, 1997; Rupert *et al.*, 1987; Schall and Simmler-Hubenthal, 1995). Recent increase in soil acidification caused by atmospheric deposition (Debicki *et al.*, 1994; Ulrich, 1990) and improper soil nutrition (Wallace, 1994) as well as an increase in alkali- and salt-affected soils (Tanji, 1995) emphasizes the need for an understanding of the mechanisms and parameters controlling soil response to pH changes. Soil reaction can alter soil structure, water and ion adsorption, acid-base equilibria, transport phenomena (Jozefaciuk *et al.*, 1993; Thomas and Hargrove, 1984) all being closely linked to the surface area of soils (Petersen *et al.*, 1996) which in turn is sensitive to changes in pH (Jozefaciuk *et al.*, 2000). To understand soil response to acid or alkali inputs better, the pH-dependent surface behavior of soil constituents *i.e.* soil minerals, among others, should be known.

Acid or alkali attack induces marked changes in the crystal structure of aluminosilicate minerals due to dissolution of structural ions and/or rearrangement of the structure. Generally, similar dissolution pathways are observed for various minerals under acid treatment involving structure destruction and formation of silicon oxides. Below pH 3 and depending on contact time, smectites delaminate and partially dissolve. Destruction of the smectite structure is connected with the removal of octahedral cations, among which Mg is the most readily removed (Christidis *et al.*, 1997). The rate of acidic dissolution of smectites increases with increasing octahedral Mg or Fe content; and the mechanism of the dissolution is independent of layer composition (Madejová *et al.*, 1998). The depopulation of the octahedral sheet of the montmorillonites may lead to different levels of structural decomposition depending on individual resistance to acid attack of the initial minerals (Breen *et al.*, 1995). The final product of acid leaching of smectites is a hydrous amorphous silica phase (Komadel *et al.*, 1990). Šucha *et al.* (2001) found that the weathering of a montmorillonite under natural conditions results in the mineral dissolution and precipitation of amorphous SiO_2. However, during the weathering of interstratified illite-smectite, the dissolution was accompanied by the appearance of smectite as a separate phase. Kaolinite on acid treatment releases preferentially the octahedral Al ions from the clay structure and forms additional Al−OH and Si−OH bonds, without disturbing the mineral structure (Suraj *et al.*, 1998).

During acid treatment of sepiolites the rearrangement of structural Si and Al atoms occurs and the clay structure is progressively transformed into amorphous silica-alumina (Dekany *et al.*, 1999). Acid treatment of a palygorskite leads to the removal of the octahedral Mg and Al, and the formation of amorphous silica from the tetrahedral sheet. The silica obtained after the treatments

* E-mail address of corresponding author:
jozefaci@demeter.ipan.lublin.pl

maintains the fibrous morphology of the natural mineral (Suárez Barrios *et al.*, 1995). Myriam (1998) found that under acid treatment, sepiolite is destroyed more rapidly than palygorskite because of its magnesian composition and larger structural microchannels. The acid attack progressively destroys the structure of saponite by partial dissolution of the octahedral Mg cations, generating amorphous silica from the tetrahedral sheet (Suárez Barrios *et al.*, 2001).

Kooyman *et al.* (1997) observed a progressive dealumination of various samples of synthetic ZSM-5 zeolites in mineral acids with increase in concentration, temperature and duration of the treatment. However, at high Al content in solution the realumination of dealuminated zeolites was observed by Sano *et al.* (1999). Among various mineral acids employed, HCl solution was the most effective for the realumination. They observed no structural degradation of HZSM-5 zeolite crystals during the acid treatment and the reinsertion of some non-framework Al in dealuminated HZSM-5 zeolites is into the framework. Natural low-silica zeolites (natrolite and thomsonite) were more reactive with acid than high-silica zeolites heulandite and stilbite. Surface-erosion of zeolite crystals was observed at a low degree of acid degradation-dissolution by Filippidis *et al.* (1996).

Usually under alkali treatment, the dissolution processes affect mineral structures to a lesser extent, though formation of new mineral phases is a frequent phenomenon. Taubald *et al.* (2000) observed that X-ray diffraction (XRD) of a smectite revealed no significant appearance or disappearance of diffraction peaks in an alkaline solution in column experiments. Higher salt concentrations in the percolating fluid inhibited the evolution of pH. Rassineux *et al.* (2001) found that the reaction of a Wyoming-type bentonite with pH 13.5 solutions at 35 and 60ºC for periods of 1 to 730 days did not alter the stability of the octahedral sheet along with the composition and the structure of the smectite layers. However, the number of expandable layers increased after octahedral charge neutralization and the number of interlayers surrounded by two charged tetrahedral sheets increased with reaction time. The particle morphology changed from flakes to hexagonal shape. More pronounced structural changes of a bentonite were observed by Ruiz *et al.* (1997) who found that the laminar structure of the starting material was converted into spherical units of the zeolitic nature by alkaline treatment in distilled and seawater media. Bauer and Velde (1999) observed that high molar KOH solutions changed the diffracting domain size of a smectite, which decreased in time, reflecting a change in crystal shape. The structure became more illite rich and the diffracting domain continued to decrease. The formation of a phillipsite from a bentonite at pH 11.7−12.6 was observed by de la Villa *et al.* (2001) in a series of closed-system hydrothermal tests at 35−90ºC. The chemistry of the equilibrium solutions, rather than the crystallization substrata, controlled the Si/Al atomic ratio and the type of zeolite formed. The decrease of Si/Al was noted at higher pH values. Illitization of a smectite in a high-pH hydrothermal environment was observed by Ylagan *et al.* (2000) and of a kaolin by Chermak and Rimstidt (1987). Baccouche *et al.* (1998) found that an interstratified illite-smectite treated with 1 to 5 mole dm^{-3} NaOH solutions on reflux for periods of 2 to 24 h formed zeolitic products. For 1 and 1.5 mole dm^{-3} NaOH solutions, zeolite Na-P1 was formed whereas for 2 to 5 mole dm^{-3} alkaline solutions, sodalite octahydrate zeolite was obtained. As a product of the reaction of natural zeolites (clinoptilolite and mordenite) with 2 mole dm^{-3} NaOH solution at 103ºC, zeolite Na-P was identified (Shin-Jyung Kang and Kazuhiko Egashira, 1997). During the reaction, a large amount of Si was dissolved into solution. Natural low-silica zeolites (natrolite and thomsonite) were more reactive with alkali as compared to the high-silica zeolites (heulandite and stilbite). Phase transformations in the base-treated low-silica zeolites to analcime were noted (Sano *et al.*, 1999).

Due to complex changes of minerals in acid or alkaline environments, their surface properties are modified. The HCl activation of two bentonites leads to a 5-fold increase of the surface area of the raw materials (Christidis *et al.*, 1997). Dekany *et al.* (1999) observed that as the amount of Fe and Al extracted from the acid-treated sepiolite increased, the specific surface area of the sample increased also. Srasra and Trabelsi-Ayedi (2000) reacted a glauconite with boiling 3 mole dm^{-3} HCl solution finding that the specific surface increased with the activation time. Natural phillipsite treated with orthophosphoric acid increased the surface area with increasing concentrations of the acid (Notario *et al.*, 1995). A palygorskite was treated with 1.0, 3.0, 5.0 and 7.0 mole dm^{-3} solutions of HCl for 1 h under reflux by Suárez Barrios *et al.* (1995). An important increase in the specific surface area was observed during the treatments, reaching a maximum in the sample treated with 5.0 mole dm^{-3} HCl. Sepiolite and palygorskite activated at different concentrations with solutions of boiling HCl under reflux conditions by Myriam (1998) showed the maximum increase in specific surface area at 3 mole dm^{-3} HCl for sepiolite and at 9 mole dm^{-3} HCl for palygorskite. For the increase in specific surface area, cleaning and disaggregation of the particles and the increase in the number of micropores were responsible. Suárez Barrios *et al.* (2001) studied the HCl activation of a saponite. Both the external and the internal surface areas of the most intensively treated sample (2.5% HCl for 24 h) were doubled with respect to that of the natural mineral. Balcı (1999) found that the BET surface area of a sepiolite increased from 150 m^2g^{-1} up to >500 m^2g^{-1} after acid treatment. Šucha *et al.* (2001) found an increase in total

surface area in a weathering profile developed on the top surface of a K-bentonite containing mixed-layer illite due to dissolution of illite-smectite and the appearance of smectite as a separate phase. However, a similar profile for Al-Mg montmorillonite showed a decrease in total surface area accompanied by montmorillonite dissolution, decrease in Mg content and precipitation of amorphous SiO_2.

Rassineux *et al.* (2001) observed a decrease of the total surface area of a Wyoming-type bentonite treated with pH 13.5 solutions at 35 and 60ºC for periods of 1 to 730 days.

As far as the authors are aware, less is known of the surface energetic properties of minerals under acid and alkali treatments. Extensively-leached clays, in which amorphous silica predominates, are considered to be hydrophobic (*i.e.* having low interaction energy with water molecules) as these catalyze reactions in non-polar media and attract non-polar reagents. Clays after short acid treatments are hydrophilic (high energy of interaction with water) as these catalyze reactions in polar media and attract polar reagents (Brown, 1994; Breen and Watson, 1998).

Generally, more is known about the surface behavior of minerals under acid than alkali treatment. The present work was designed to compare the effects of both treatments on surface areas and adsorption energies of selected minerals, which are most abundant in soils.

MATERIALS AND METHODS

Bentonite (Chmielnik, Poland), biotite (Chongyang, Korea), illite (Yongdong, Korea), kaolin (Vimianzo, Spain), vermiculite (Lovec, Bulgaria) and zeolite (Wolsong, Korea) were studied. The minerals were treated for 2 weeks at room temperature with hydrochloric acid or sodium hydroxide solutions of 0.10, 1.0 and 5.0 mole dm^{-3} at 1:50 solid:liquid ratio. The control samples were treated with distilled water. The treatment suspensions were shaken occasionally. After the first week, the treatment solutions were renewed. After treatments, the solids were washed intensively with 1 mole dm^{-3} NaCl solution by centrifuging. Because surface properties of minerals depend strongly on ionic composition (Cases *et al.*, 1997; Hall and Astill, 1989; Keenan *et al.*, 1951) the samples were transferred to calcium homoionic forms by triple 1 mole dm^{-3} $CaCl_2$ treatment followed by washing of excess salt to the negative reaction of the supernatant liquid with $AgNO_3$. Finally the samples were air dried and gently powdered in a mortar.

All treatment solutions were collected and analyzed using inductively coupled plasma atomic emission spectrometry (ICP-AES) for the dissolved elements Al, Ca, Fe, K, Mg and Si.

The XRD patterns were recorded using DRON-3 apparatus (CuKα radiation). The minerals were identified using data from Thorez (1976).

Nitrogen adsorption isotherms were measured in duplicate at liquid nitrogen temperature using a Carlo Erba Sorptomatic 1990. Taking into account that the differences between the two replicates were very small (<0.4%), we decided not to repeat the measurement because of the high costs of analysis.

Water vapor adsorption isotherms were measured in triplicate using the vacuum chamber method at the temperature T = 294±0.1 K. Gently-ground samples were placed as ~2 mm thick layers in weighing vessels and closed in the chamber. The pressure in the chamber was reduced to ~100 Pa. The relative water vapor pressure, P/P_0, in the chamber was controlled by sulfuric acid solutions of step-wise decreasing concentrations (increase of the P/P_0). The amount of adsorbed water at a given P/P_0, a(kg/kg), was measured by weighing after 48 h of equilibration. The dry mass of the samples was estimated after completing adsorption measurements, after 24 h oven drying at 378 K. During the drying, heated dry nitrogen was pumped through the oven. The differences between triplicate measurements of the isotherms did not exceed 1.7%.

We assumed that the drying procedure applied removed physically adsorbed water (Cases *et al*., 1997). This does not necessarily mean that the minerals are fully dehydrated, *e.g.* drying of a montmorillonite at temperatures between 100 and 500ºC results in the removal of water molecules linked to the exchangeable cations. This kind of water can account for ~3% of the final mass. At higher temperatures, the further loss of ~5% of the final mass represents dehydroxylation of the structure (Cases *et al*., 1997). In our experiments we did not perform more severe dehydration of the minerals, because the removal of water molecules bound with higher energies can lead to results which are not describable by the model of physical adsorption used in this paper.

Surface area values were calculated from adsorption data using the linear form of the Aranovich (1992) isotherm:

$$x/[a(1 - x)^{1/2}] = 1/(a_m C) + x/a_m \quad (1)$$

where $x = P/P_0$, a_m (kg/kg) is the statistical monolayer capacity and $C = \exp((E_a\text{-}E_c)/RT)$ is the constant related to the adsorption energy, E_a (J), and condensation energy of water, E_c (J). In contrast to the standard Brunauer-Emmett-Teller (BET) model (Brunauer *et al.*, 1938), the Aranovich isotherm allows for the presence of vacancies in the adsorbed layer and fits the experimental polymolecular adsorption data over a broader range of relative pressures (~0.05 < P/P_0 < 0.8) than the BET does (~0.05 < P/P_0 < 0.35). After calculating a_m values from the slopes of the linearity range of equation 1, the surface areas of the samples were calculated as:

$$S = L\omega a_m/M \quad (2)$$

where L is the Avogadro number, M is molecular mass of the adsorbate and ω is the area occupied by a single

adsorbate molecule. The ω value for water was taken as 1.08×10^{-19} m^2 and for nitrogen as 1.62×10^{-19} m^2 (Gregg and Sing, 1967). In two cases (water adsorption on biotite and vermiculite), where the adsorption data plotted within the linear coordinates of the Aranovich isotherm (equation 1) gave no satisfactory linear fit, we calculated the monolayer capacity, using the formula:

$$a_m = \max\{a(1 - x)^{1/2}\} \quad (3)$$

The monolayer capacities calculated using equations 1 and 3 were very close to each other for the other minerals studied.

According to the theory of adsorption on heterogeneous surfaces (Jaroniec *et al.*, 1975; Jaroniec and Brauer, 1986; Rudzinski *et al.*, 1982) the total adsorption at a given pressure P can be expressed as a sum of local adsorptions a_i on given sites of energy $E_i = (E_{a,i} - E_c)$, where $E_{a,i}$ is adsorption energy of i-th site:

$$a(P) = \sum_{i=1}^{n} a_i(P,E_i) \quad (4)$$

Thus the total adsorption isotherm, $\Theta_\tau(P)$, can be written as a sum of adsorptions on each sites, $\Theta_i(P,E_i)$, weighted by their fractions, $f(E_i)$:

$$\Theta_\tau(P) = a(P)/a_m = \sum_{i=1}^{n} a_i(P,E_i)/a_{m,i}(a_{m,i}/a_m) = \sum_{i=1}^{n} \Theta_i(P,E_i) f(E_i) \quad (5)$$

where $a_{m,i}$ is the monolayer capacity of sites of kind i and values of $f(E_i)$ fulfil a normalization condition:

$$\sum_{i=1}^{n} f(E_i) = 1 \quad (6)$$

If the local adsorption isotherm in equation 4 is expressed by the Aranovich equation, one has:

$$\Theta_\tau(P) = (1 - x)^{-1/2} \sum_{i=1}^{n} C_i x/(1 - C_i x) f(E_i) \quad (7)$$

where C_i is the value of the constant C of sites of kind i.

Solving equation 7 with respect to $f(E_i)$ is a difficult problem. A small variation in experimental data can cause a large variation in estimation of site fractions. A method which is less sensitive to experimental error, is reasonably accurate and provides a convenient way to overcome this problem is to apply a condensation approximation CA (Cerofolini, 1974; Harris, 1968, 1969). This method is based on the replacement of the true local isotherm by a step function. Every pressure value becomes associated with the corresponding value of the adsorption energy which provides the adsorption equal to half of the adsorption at infinite energy. Following this definition, the final formula for calculation of site fractions is:

$$f(E_i) = [(1 - x_{i+1})^{1/2} \Theta_\tau(E_{i+1}) - (1 - x_i)^{1/2} \Theta_\tau(E_i)]/(E_{i+1} - E_i) \quad (8)$$

From $f(E_i)$ values, the average water vapor adsorption energy, E_{av}, can be calculated as:

$$E_{av} = \sum_{i=1}^{n} E_i f(E_i) \quad (9)$$

More details on the above calculations can be found in Jozefaciuk and Shin (1996).

The calculation of adsorption energy distribution functions ($f(E_i)$ against E_i dependencies) was performed using equation 8. Energy values were expressed in units of thermal energy, RT. The scaled energy, $(E_a - E_c)$/RT, ranging from 0 to −8 was considered. The scaled energy equal to 0 holds for energy adsorption equal to the condensation energy of the vapor. The value of −8 was taken as the maximum adsorption energy. The maximum energy value in the condensation approximation should relate to the minimum value of the P/P_0 applied. The minimum relative pressure in our water vapor adsorption data sets was ~0.004, which corresponds to the energy adsorption of around −5.5. Thus it was reasonable to assume −6 as the maximum energy in the present investigations. However, this value can be considered only as a first estimate of the maximum energy because of the lack of experimental data at lower relative pressures. We arbitrarily set the maximum energy to −8 in the belief that if there were no sites with higher adsorption energies than −6 then the corresponding values of $f(E_i)$ will be close or equal to zero. Providing sufficient precision for the estimation of energy distribution functions for the replicates of water adsorption data required the detection of the adsorbing sites differing at least by two energy units. The value of adsorption (Θ_τ) at a given energy was found by linear interpolation of the nearest experimental adsorption data. Although the nitrogen adsorption data were more precise and started at lower P/P_0 values, for easier comparison of the results, the nitrogen adsorption energy distribution functions were calculated by applying the same restrictions. Having $f(E_i)$ values, average adsorption energies were calculated from equation 9.

RESULTS AND DISCUSSION

The amounts of the dissolved elements during acid and alkali treatments of the studied minerals are presented in Table 1. All elements except Si dissolved better in acidic than in alkaline media. However, excluding biotite and vermiculite, the total amount of the dissolved solid was greater in 5 N NaOH than in 5 N HCl, due to extreme Si dissolution. Very high individual differences in the dissolution patterns of the minerals can be seen.

The XRD patterns of the studied minerals are presented in Figure 1. Frequently the alkali treatment leads to sharpening of the basal reflections, which may be due to the dissolution of most irregular (amorphous) mineral particles (cleaning of the minerals). Taking into account large amounts of Si dissolved in alkaline media, removal of outer silica sheets of the minerals can also occur. As a rule, the acid treatment leads to severe alteration of the crystal structure of the minerals which is seen from lowering and broadening of the character-

Table 1. Dissolution of the studied minerals under acid and alkali treatment. The data show amounts (mg) of elements dissolved from 1 g of the mineral (average from three replicates).

Treatment*	Elements dissolved (mg g^{-1}) Al	Ca	Fe	K	Mg	Si	SD (%)
Bentonite							
5 M HCl	7.03	17.85	4.23	7.74	2.77	6.82	7.24
1 M HCl	1.27	13.51	1.26	1.89	1.47	4.98	3.74
0.1 M HCl	0.25	1.98	0.029	0.53	0.14	1.32	0.67
Control	0.011	0.3	0.0004	0.25	0.06	0.29	0.14
0.1 M NaOH	0.1	0.56	0.024	0.17	0.02	3.46	0.77
1 M NaOH	0.31	0.14	0.011	0.92	0.0	12.6	2.55
5 M NaOH	1.88	0.12	0.059	1.63	0.0	35.7	7.23
Biotite							
5 M HCl	22.1	10	27.1	24.6	45.2	4.72	21.3
1 M HCl	6.39	9.6	8.54	9.59	13.44	6.46	8.55
0.1 M HCl	0.09	3.19	1.01	3.85	1.08	0.81	1.48
Control	0.001	0.42	0.0005	0.23	0.021	0.031	0.10
0.1 M NaOH	0.025	0.071	0.016	0.54	0.039	0.29	0.15
1 M NaOH	0.102	0.21	0.013	1.02	0.066	1.0	0.39
5 M NaOH	1.02	0.83	0.042	3.81	0.032	12.56	3.19
Illite							
5 M HCl	1.36	1.02	4.41	0.98	0.042	1.19	1.40
1 M HCl	0.88	0.84	1.45	0.89	0.004	0.64	0.74
0.1 M HCl	0.52	0.85	0.37	0.69	0.005	0.37	0.44
Control	0.002	0.57	0.001	0.077	0.004	0.04	0.10
0.1 M NaOH	0.4	0.03	0.014	0.325	0.032	0.51	0.23
1 M NaOH	0.84	0.04	0.038	0.494	0.077	1.54	0.54
5 M NaOH	2.34	0.13	0.077	1.765	0.035	15.6	3.62
Kaolin							
5 M HCl	8.15	4.93	1.904	0.595	0.93	3.12	3.32
1 M HCl	3.64	3.57	0.577	0.158	0.35	3.09	1.92
0.1 M HCl	0.81	2.44	0.023	0.059	0.1	1.7	0.84
Control	0.007	0.13	0.0002	0.038	0.015	0.06	0.04
0.1 M NaOH	0.808	0.049	0.008	0.434	0.034	1.02	0.42
1 M NaOH	2.99	0.048	0.013	0.987	0.079	3.99	1.47
5 M NaOH	16.03	0.199	0.042	2.74	0.047	19.7	7.11
Vermiculite							
5 M HCl	28.61	28.71	18.25	11.21	22.43	12.58	19.66
1 M HCl	4.97	24.36	1.75	1.51	15.82	5.27	8.41
0.1 M HCl	0.18	3.81	0.006	0.5	0.83	0.72	0.91
Control	0.015	0.06	0.0003	0.05	0.42	0.058	0.10
0.1 M NaOH	0.108	0.34	0.0031	0.7	0.039	0.82	0.33
1 M NaOH	0.239	0.27	0.025	0.86	0.016	2.33	0.64
5 M NaOH	0.955	0.58	0.045	0.79	0.0	15.71	3.29
Zeolite							
5 M HCl	17.8	14.6	5.91	4.93	1.95	3.62	7.93
1 M HCl	11.3	11.6	1.96	1.24	1.21	2.06	4.80
0.1 M HCl	0.24	6.31	0.06	0.14	0.17	0.82	1.14
Control	0.0	1.85	0.001	0.09	0.0	0.22	0.31
0.1 M NaOH	0.0	0.41	0.007	0.44	0.01	2.59	0.60
1 M NaOH	0.68	0.17	0.004	0.74	0.0	4.18	1.03
5 M NaOH	5.88	0.53	0.056	3.05	0.0	41.0	9.22

Abbreviations: * the letter M denotes mole dm^{-3}; SD (%) is w/w percentage of solid dissolved (sum of dissolved elements as oxides expressed as the percentage of the mass of the initial mineral).

istic peaks on the patterns, indicating a decrease in the regularity of the mineral structure. An increase in the diffraction intensity at very low angles can be due to the dispersion and amorphization of the minerals. The XRD patterns and the qualitative composition of dissolved elements for the bentonite can indicate that the destruction of the smectite crystallites during acid attack goes through interlamellar cation depletion and dissolution of the crystal structure which leads to dispersion and amorphization of the mineral. In the biotite, after both

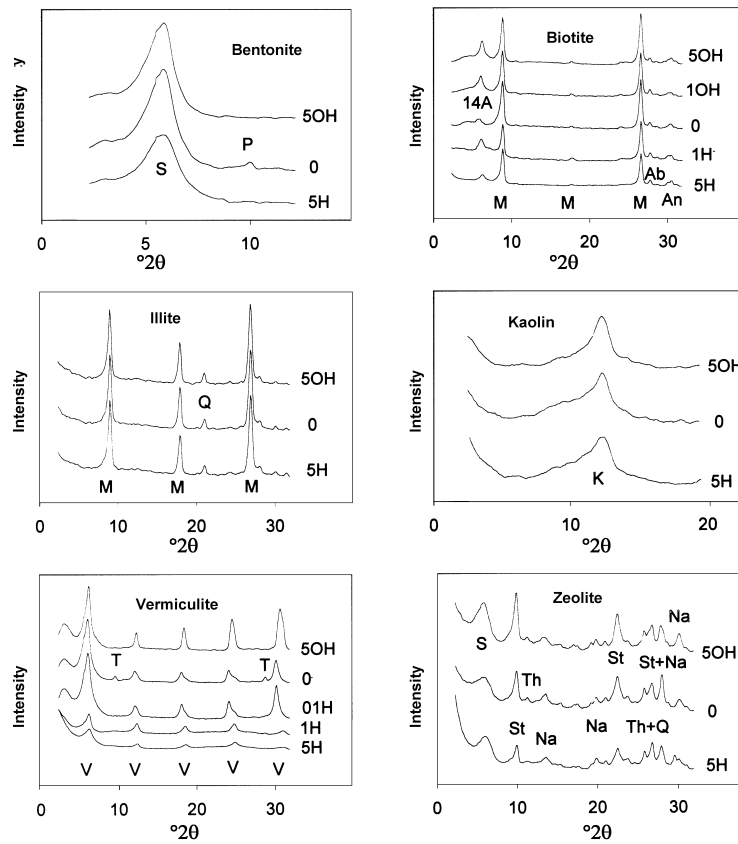

Figure 1. XRD patterns for the studied minerals. Abbreviation: Ab – albite, An – anorthite, K – kaolinite, M – mica, Na – natrolite, P – paragonite, Q – quartz, S – smectite, St – stilbite, T – talc, Th – thompsonite, V – vermiculite. Acid and alkali treatments are marked as 5H for 5 N HCl, 5OH for 5 N NaOH etc.

treatments, a new, 14 Å peak (2θ =7º) arises, which is practically absent in the untreated mineral, indicating formation expansible phases. Such structures formed in biotites via non-exchangeable K depletion (note high K dissolution from the studied biotite, Table 1) are accompanied by interlamellar expansion (Fanning *et al.*, 1989). Formation of similar structures in weathered biotite flakes was also found by electron microscope observations (Boyle *et al.*, 1967). Kaolin and illite seem to be most resistant to acid and alkali attack. The intensity of all basal XRD reflections of the vermiculite decreased sharply under acid attack indicating that not only the octahedral but also the tetrahedral sheets undergo severe alteration. The latter phenomenon can be also connected with high Si dissolution. The presence of mobile octahedral Mg and FeII ions in the vermiculite is a reason for its easy destruction. The zeolite used was not a pure mineral, though amorphization of its components is seen from the XRD spectra.

Adsorption isotherms for the studied minerals are shown in Figure 2. All nitrogen and most water adsorption isotherms are of the 2nd type (S-shaped) BET classification. Water vapor adsorption isotherms on biotite and vermiculite (except 1 N and 5 N HCl-treated vermiculite) at low relative pressures (P/P_0 < 0.4) resemble a combination of two Langmuir-type isotherms and the adsorption at medium relative pressures (0.4 < P/P_0 < 0.8) seems to be strongly limited. In general the adsorption of water and nitrogen increased with the increase in concentration of both treatments, though a few of the control samples adsorbed more vapor than those treated with low concentrations of acid or alkali. The increase in adsorption was usually much higher under acidic than under alkaline treatments.

The surface areas of the control minerals are shown in Table 2. Usually the data in the literature refer to the surface area of the minerals calculated using the BET model. The Aranovich model used in this paper gives

Table 2. Surface areas S and scaled adsorption energies $E_{av} = (E_a - E_c)/RT$ of the control samples of the minerals studied.

Mineral	S, nitrogen (m^2g^{-1})	S, water (m^2g^{-1})	E_{av}, nitrogen	E_{av}, water
Bentonite	38.4	311	−5.1	−3.2
Biotite	9.1	26.3	−2.9	−3.8
Illite	25.6	38.0	−2.8	−5.2
Kaolin	14.2	48.1	−3.8	−2.3
Vermiculite	13.2	352	−3.0	−1.8
Zeolite	13.5	133	−5.4	−3.1

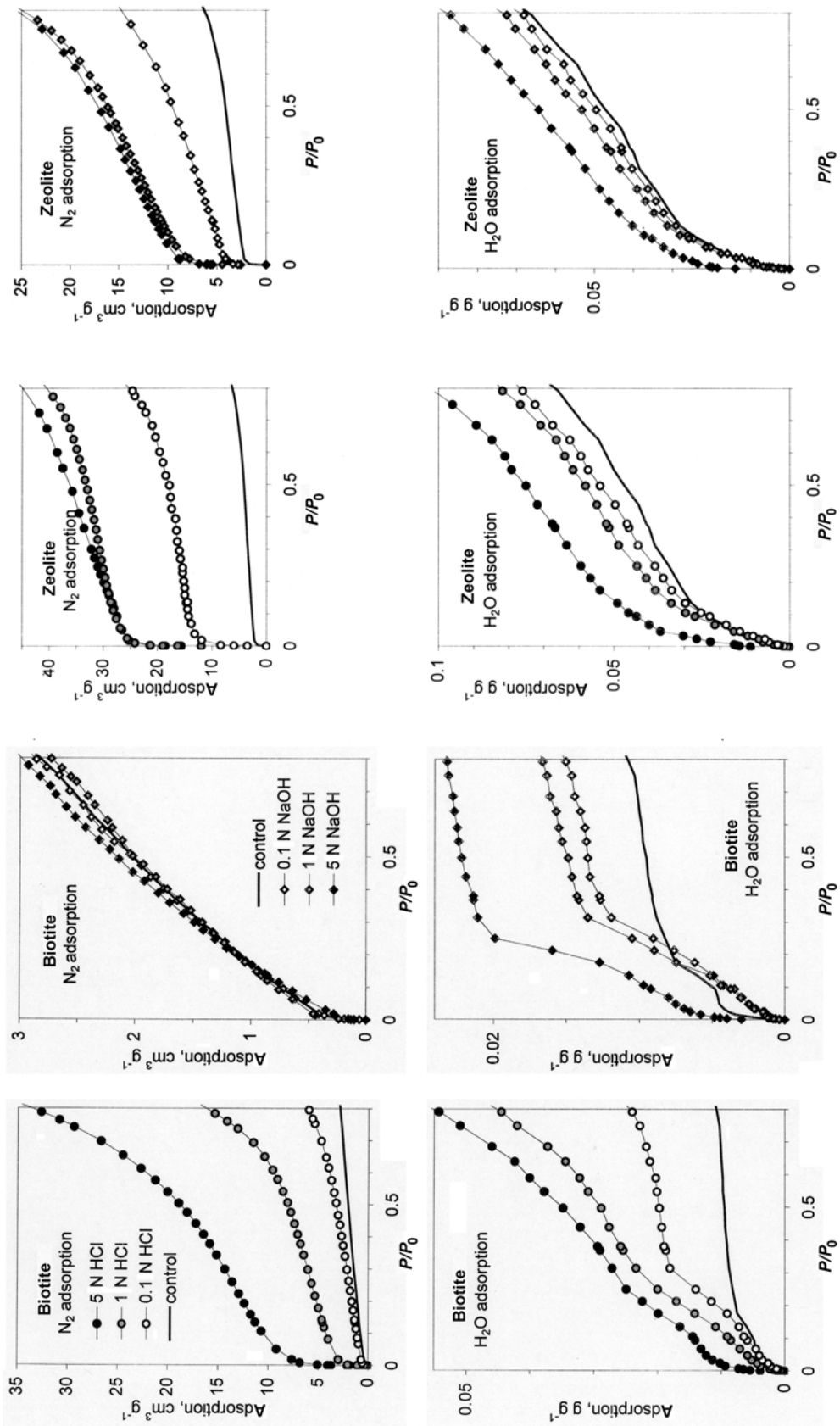

Figure 2. Nitrogen and water vapor adsorption isotherms for acid- and alkali-treated minerals.

surface areas ~25% larger. Throughout the literature (cited papers), the lowest surface areas are reported for kaolinites: from 5 to 25 (nitrogen) and 10 to 30 m^2g^{-1} (water). Surface areas of illites from 50 to 200, of zeolites from 100 to 400 and for vermiculites up to 700 m^2g^{-1} are found (Newman, 1987; Moise *et al*., 2001; Volzone *et al*., 1999). For smectites, surface areas of 110−550 m^2g^{-1} are found from water adsorption and 80−180 m^2g^{-1} from nitrogen adsorption, however a surface area nitrogen as low as 14 m^2g^{-1} was found in a montmorillonite extracted from Kuzmice bentonite (Czech Republic) by Tombacz *et al*. (1998). Extremely high surface areas of smectites, ~800 m^2g^{-1} are measured using ethylene glycol monoethyl ether (EGME) sorption, being close to the value determined from the crystallographic cell dimensions and weight (Van Olphen, 1997). The EGME method is based upon equilibration of the exhaustively dehydrated mineral with the reagent vapor at a single value of the vapor pressure. The single-point adsorption rarely meets these experimental conditions at which neither more nor less than the effective monolayer is formed. If the sample is exhaustively dehydrated and water is removed from non-physical adsorption centers, the ethylene glycol may solvate these centers leading to improbably high readings of the amount adsorbed.

Frequently the nitrogen surface area has been interpreted as the 'external' surface, and the water surface area as the 'total' one, including the external and internal (interlayer) surfaces. In most cases the total surface area exceeding the external one is measured. As seen from Table 2, for all of the original minerals, the water surface area is greater than the nitrogen surface area: for bentonite and zeolite about 10 times, for vermiculite more than 25 times, whereas for the other minerals ~2−3 times. Such large differences may arise not only from the differences between the external and the total surface areas. The nitrogen adsorption method requires prior evacuation and heating of the sample, thereby thinning water films and bringing the clay particles closer. The quasi-contact of the mineral plates (for morphological platy clays) can extend over a significant portion of the surface, which becomes inaccessible for non-polar (nitrogen) molecules. If the clay contains expansible interlayers, these collapse on evacuation, giving the same effect. The molecular sieving is believed to differentiate the entrance of gas molecules of various sizes into narrow spaces (Volzone *et al.*, 1999) leading to differences in surface area. The kinetic effects may diminish the adsorption of nitrogen to a great extent when entrances to larger spaces are of nitrogen molecule dimensions. To pass such a narrow entrance easily, the thermal energy of the molecule should be similar to the energy barrier of the adsorption field among the entrance walls. At liquid nitrogen temperature the thermal energy is low and therefore the adsorption equilibrium may not be reached within a standard time of the measurement. Many restrictions hold also for interpretation of water surface area as a total mineral surface, among which is different hydration of different surface cations, strong lateral interaction of polar water particles in adsorbed layer and/or different water content in interlayers at a point of the statistical monolayer coverage (*i.e.* single water layer in interlayers of high charge density clays and double layer in low charge density clays). Comprehensive discussions on nitrogen and water adsorption interpretation are presented by Gregg and Sing (1967), Newman (1985) and Low (1961).

Changes in the surface area of the studied minerals during acid and alkali treatments are shown in Figure 3 where the ratio of the surface area of the treated mineral to the surface area of the control sample is given. Note that parts of the curves depicting extreme changes (dashed lines) are not proportional to the others and the shifted points are labeled with their real values. Except for the nitrogen surface area for acid-treated illite and alkali-treated bentonite and vermiculite, the surface areas of the studied minerals increased generally with both acid and alkali treatments. However, in a few cases

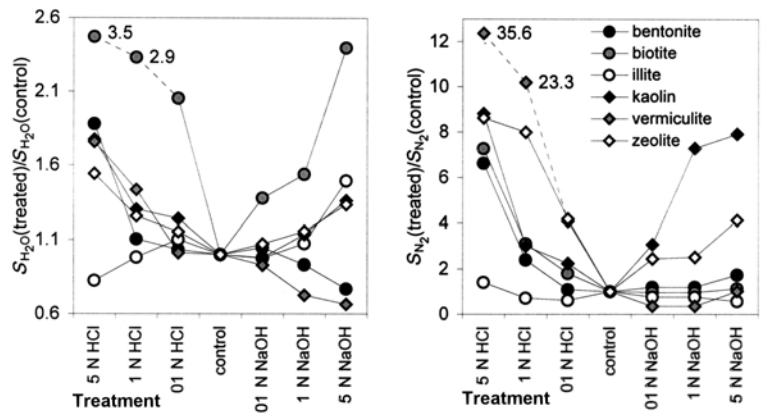

Figure 3. Relative changes in surface areas due to the treatments. On the *y* axis the ratio of the control sample surface to that of the treated sample is given. The points which are shifted against the *y* axis are labeled with their real values.

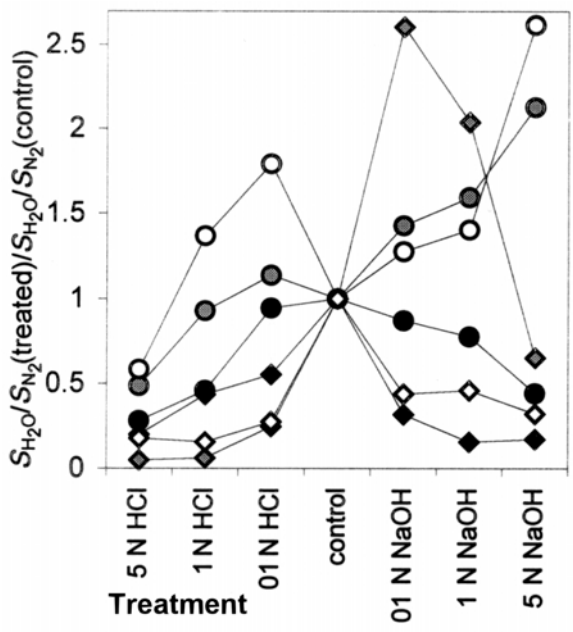

Figure 4. Relative changes in ratio of water surface area to nitrogen surface area due to the treatments. Symbols as for Figure 3.

the surface area decreases after the lowest treatment concentration. This may be due to the removal of the minerals' impurities, *e.g.* amorphous and/or very finely dispersed crystalline solids having very high surface areas. The acid treatment affects surface areas more than the alkaline treatment. The nitrogen surface areas are more sensitive to the treatments. For example, at the highest acid treatment the nitrogen surface area of vermiculite increased up to 35 times whereas the water surface area increased by less than a factor of 2. The greatest increase of the water surface area after both acid and alkali treatments occurred for the biotite, which may reflect the adsorption in newly-formed expanded layers. The increase of the surface area under acid treatment may be caused by production of finely dispersed silicon oxides from destruction of mineral structures, removal of amorphous Al or silica components plugging surface pores or interlamellar spaces, formation of the surface cracks and voids. Under alkaline conditions, similar processes may occur together with an accumulation of Fe and Mg hydroxides (Ca hydroxides were probably dissolved during the washing step). A large value for the surface area is important for catalytic activity of acid-activated clays. The alkaline treatment producing high surface areas may possibly be used in production of the mineral catalysts as well.

With the exception of alkali-treated biotite and illite, the increase of the concentration of both treatments led to a smaller increase of the water surface area than the nitrogen surface area, which is explicitly presented in Figure 4 showing the ratio of these two values. That the increase of both nitrogen and water surface areas is not parallel may be caused by opening of N_2 inaccessible spaces, as well as by formation of new adsorbents on which nitrogen adsorption is greater than that of water. These can include various silicon oxides having higher nitrogen than water surface area (Gregg and Sing, 1967). An occurrence of silicon oxides after alkali treatment seems less probable. Short-term alkali treatment (hot NaOH) is supposed to clean mineral surfaces of silicon oxides, which is frequently applied as one of the pre-treatment steps for mineralogical XRD analysis (Kunze and Jackson, 1965). Silicon compounds are more soluble under alkaline conditions than *e.g.* Fe or Mg; thus under long-term treatment, the latter phases (if any) may affect changes in surface areas.

Average adsorption energy values of the original minerals are included in Table 2. Biotite and illite have higher water than nitrogen adsorption energy, whereas for the other minerals the opposite was found. Changes of average adsorption energies under acid and alkali treatments are presented in Figure 5, constructed in a similar fashion to Figures 3 and 4. With the increase of acid treatment concentration, the average water adsorption energy increases for biotite and zeolite and decreases for bentonite, illite and kaolin, whereas the nitrogen adsorption energy increases in most cases. The

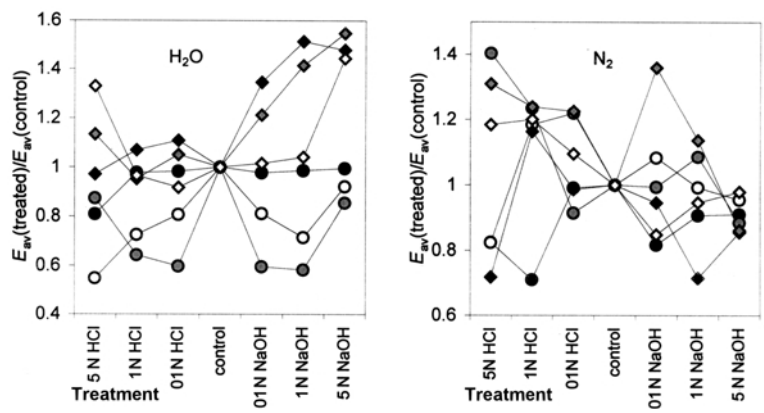

Figure 5. Relative changes in average adsorption energies due to the treatments. Symbols as for Figure 3.

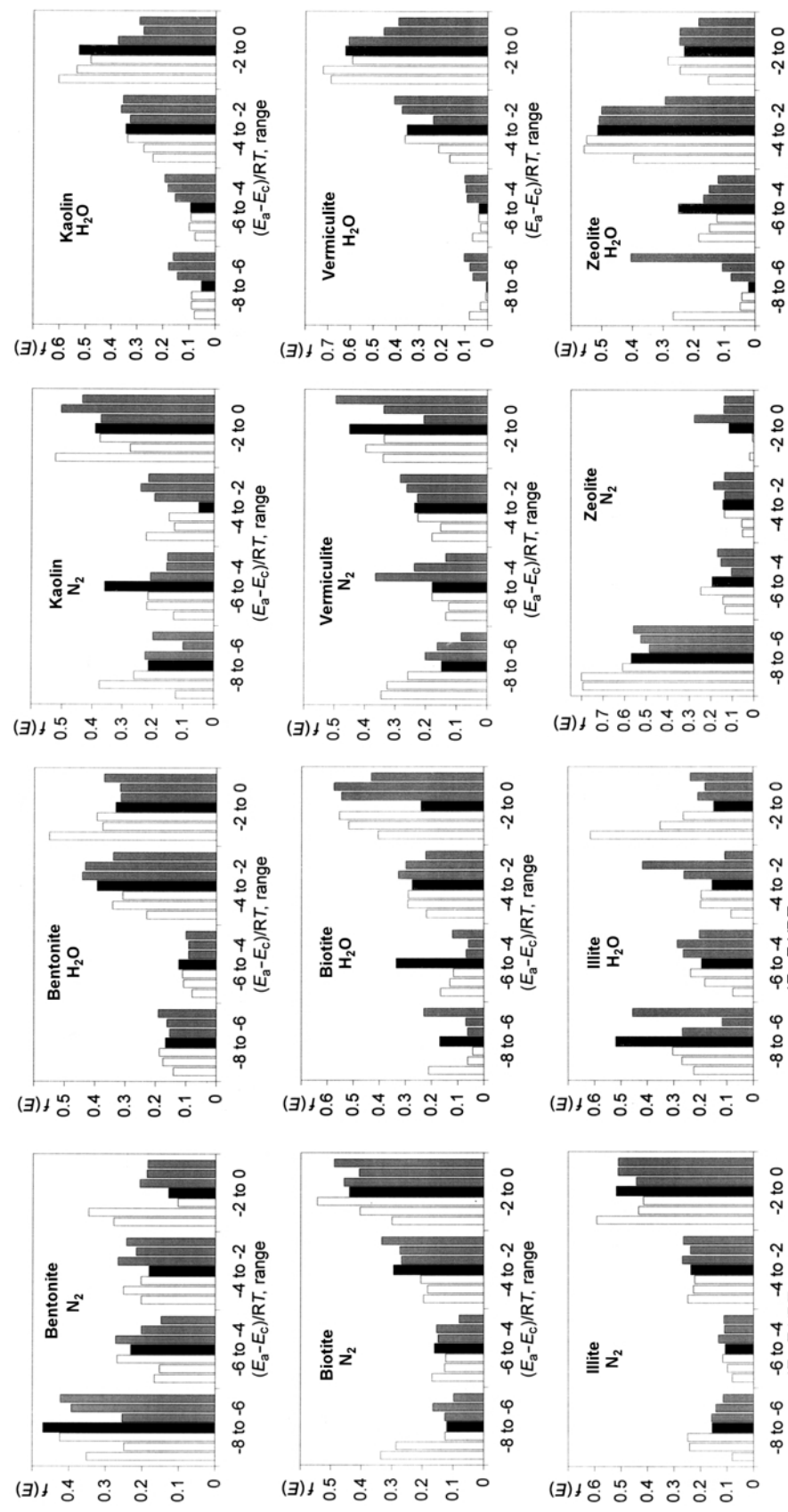

Figure 6. Nitrogen and water vapor adsorption energy distribution functions for the minerals before and after treatments. Black bars – untreated samples, white bars – acid-treated, gray bars – alkali-treated. Within a given energy range, the higher the treatment concentration, the higher the distance from the black bar.

increase in adsorption energy may be due to the formation of cracks and voids on the surfaces attacked. The decrease in adsorption energy may be due to the removal of surface impurities. Silicon oxides, products of mineral destruction, also have low adsorption energy (Gregg and Sing, 1967). Changes of the nitrogen adsorption energies under alkali treatment appear to follow the opposite direction to that of the water adsorption energies, which can reflect different polarity of the adsorbates and different forces involved in their interactions with surfaces.

The nitrogen and water adsorption energy distribution functions and their changes under the treatments are shown in Figure 6. Because the condensation approximation used for evaluation of energy distribution functions is considered to be precise only at 0 K (Rudzinski and Everett, 1991), one can suspect that the nitrogen adsorption distribution is more realistic because of the low temperature of measurement. However, the energy distribution function characterizes the adsorbent-adsorbate system thus reflecting also the different polarity of adsorbate molecules. Anyway, both adsorption energy distributions and especially that of the water vapor should be used for comparison between particular minerals and treatments and not as absolute surface characteristics.

The nitrogen adsorption energy distribution functions of original bentonite and zeolite have dominant high-energy peaks (−8 to −6 E/RT range) showing that the nitrogen adsorption process is highly energetic. In the water vapor adsorption energy distribution functions of these minerals, lower energy peaks (−4 to −2 E/RT range) dominate, indicating that water molecules undergo adsorption with lower energies, consistent with the latter conclusion. The adsorption of nitrogen on original biotite, illite and vermiculite is at low energy: the 0 to −2 E/RT peak dominates and with increasing energy adsorption, consecutively smaller site fractions occur. In the water vapor energy distribution function of biotite, the −6 to −4 E/RT sites dominate. The shape of this function for illite is a mirror reflection of its nitrogen adsorption distribution function. For vermiculite, both water and nitrogen adsorption energy distributions are similar, though a very small fraction of high-energy (−8 to −4 E/RT) sites occurs for water adsorption. The nitrogen adsorption distribution function for kaolin is bimodal with two peaks of −6 to −4 and −2 to 0 E/RT sites, whereas water adsorption reveals higher inputs of lower energy peaks. Individual minerals apparently have different, mineral-specific surface adsorption sites.

Changes in nitrogen and water adsorption energy distribution functions under the treatments (Figure 6) appear to exhibit no common tendencies for all minerals. Assuming that during the lowest-concentration treatments the mineral surfaces are 'cleaned' of impurities, changes in fractions of different energy sites starting from 0.1 N treatments can better reflect alterations of mineral surfaces under acid and base attack. However, well-defined common trends are also lacking. For example, an increase of highly energetic adsorption sites (E/RT between −8 and −6) occurs for acid-treated vermiculite, zeolite and biotite, whereas the fraction of these sites seems to decrease for illite.

Acid-treated minerals should be generally less polar than those treated with alkali, due to the formation of low energetic silica from mineral lattice destruction. Alkali-treated minerals should be more polar due to eventual formation of finely dispersed and highly energetic Mg or Fe oxide precipitates and/or removal of outer silica sheets from mineral structures leaving alumina sheets more polar than silica. Together with producing chemically different surface groups and energetic centers in individual minerals, acid and alkali attack may change the geometrical surface features, which can affect the adsorption energies and site distribution functions. Chemically identical surfaces may exhibit different adsorption energies depending on their shape, *e.g.* by overlapping of force field between fine pore walls, thus increasing adsorption potential. Different directions and/or intensities in changes in surface/micropore structure for individual minerals may lead to a lack of general patterns in the behavior of distinct adsorption sites observed for the minerals studied, even at the same level of treatment.

CONCLUSIONS

An increase in surface area was observed for all the minerals studied under both acid and alkali treatments carried out at room temperature over 2 weeks. With increasing reagent concentration, the nitrogen surface area increased faster than the water surface area. In acid treatments, dissolution of Al prevailed over that of Si but the opposite was observed in alkali treatments. Different polarities of the treated minerals were reached due to different energetic features of the resulting surfaces. Illite and kaolin were the most resistant to acid attack.

Because the surface properties of clay minerals and surface area in particular are very sensitive to acid and alkali attack, the surface properties of soil clay fractions might possibly be used to monitor processes accompanying changes in soil reactions.

ACKNOWLEDGMENTS

The authors are grateful to Dr Tatiana Alekseeva and Dr Andrey Alekseev from the Institute of Basic Problems of Soil Science, Puschino, Russia for recording and interpreting the XRD patterns.

REFERENCES

Aranovich, G.L. (1992) The theory of polymolecular adsorption. *Langmuir*, **8**, 736–739.

Baccouche, A., Srasra, E. and El Maaoui, M. (1998)

Preparation of Na-P1 and sodalite octahydrate zeolites from interstratified illite-smectite. *Applied Clay Science*, **13**, 255–273.

Balcı, S. (1999) Effect of heating and acid pre-treatment on pore size distribution of sepiolite. *Clay Minerals*, **34**, 647–653.

Bandosz, T.J., Jagiello, J., Andersen, B. and Schwartz, J.A. (1992) Inverse gas chromatography study of modified smectite surfaces. *Clays and Clay Minerals*, **40**, 306–310.

Bauer, A. and Velde, B. (1999) Smectite transformation in high molar KOH solutions. *Clay Minerals*, **34**, 259 – 273.

Bergaya F. and Lagaly G., (2001) Surface modification of clay minerals. *Applied Clay Science*, **19**, 1–3.

Boyle, J.R., Voigt, G.K. and Sawhney, B.L. (1967) Biotite flakes: Alteration by chemical and biological treatment. *Science*, **155**, 193–195.

Breen, C. and Watson, R. (1998) Acid-activated organoclays: preparation, characterisation and catalytic activity of poly-cation-treated bentonites. *Applied Clay Science*, **12**, 479–494.

Breen, C., Madejová, J. and Komadel, P. (1995) Correlation of catalytic activity with infra-red, ^{29}Si MAS NMR and acidity data for HCl-treated fine fractions of montmorillonites. *Applied Clay Science*, **10**, 219–230.

Brown, D.R. (1994) Clays as catalysts and reagent supports. *Geologica Carpathica - Clays,* **45**, 45–56.

Brown, D. and Rhodes, C.N. (1995) Acid-treated and ion exchanged montmorillonite catalysts: dependence of activity on composition. Pp. 189–190 in: *Clay and Clay Material Sciences, Proceedings of Euroclay'95, Leuwen* (A. Elsen, P. Grobet, M. Keung, H. Lehman, R. Schoonheydt and H. Toufar, editors).

Brunauer, S., Emmet, P.H. and Teller, E. (1938) Adsorption of gases in multimolecular layers. *Journal of American Chemical Society*, **60**, 309–314.

Cases, J.M., Berend, I., Francois, M., Uriot, J.P., Michot, L.J. and Thomas, F. (1997) Mechanism of adsorption and desorption of water vapor by homoionic montmorillonite. 3. The Mg, Ca, Sr, and Ba exchanged forms. *Clays and Clay Minerals*, **45**, 8–22.

Cerofolini, G.F. (1974) Localized adsorption on heterogeneous surfaces. *Thin Solid Films*, **23**, 129–152.

Chermak, J.A. and Rimstidt, J.D. (1987) The hydrothermal transformation of kaolinite to muscovite/illlite. *Geochimica et Cosmochimica Acta,* **54**, 2979–2990.

Christidis, G.E., Scott, P.W. and Dunham, A.C. (1997) Acid activation and bleaching capacity of bentonites from the islands of Milos and Chios, Aegean, Greece. *Applied Clay Science*, **12**, 329–347.

de la Villa, R.V., Cuevas, J., Ramirez, S. and Leguey, S. (2001) Zeolite formation during the alkaline reaction of bentonite. *European Journal of Mineralogy*, **13**, 635–644.

Debicki, R., Filipek, T., Glinski, J. and Sikora, E., editors (1994) Natural and anthropogenic causes and effects of soil acidification. *Zeszyty Problemowe Postepow Nauk Rolniczych*, **413**, 1–334.

Dekany, I., Turi, L., Fonseca, A. and Nagy, J.B. (1999) The structure of acid treated sepiolites: small-angle X-ray scattering and multi MAS-NMR investigations. *Applied Clay Science*, **14**, 141–160.

Drief, A., Nieto, F. and Sanchez-Navas, A. (2001) Experimental clay-mineral formation from a subvolcanic rock by interaction with 1 mole dm^{-3} NaOH solution at room temperature. *Clays and Clay Minerals*, **49**, 92–106.

Eberl, D.D., Velde, B. and McCormick, T. (1993) Synthesis of illite-smectite from smectite at earth surface temperatures and high pH. *Clay Minerals*, **28**, 49–60.

Fanning D.S., Keramidas V.Z. and El-Desosky M.A. (1989) Micas. Pp. 527–634 in: *Minerals in Soil Environments* 2nd edition (J.B. Dixon and S.B. Weed, editors). SSSA Book Series **1**. Soil Science Society of America, Madison, Wisconsin.

Filippidis, A., Godelitsas A., Charistos, D., Misaelides, P. and Kassoli-Fournaraki, A. (1996) The chemical behavior of natural zeolites in aqueous environments: Interactions between low-silica zeolites and 1 mole dm^{-3} NaCl solutions of different initial pH-values. *Applied Clay Science*, **11**, 199–209.

Frank, U. and Gebhardt, H. (1991) Weathering of silicates and destruction of clay minerals as a consequence of severe soil acidification in selected forest locations of Northern Germany. *Proceedings of the 14th International Congress of Soil Science*, Kyoto, **VII**, 61–65.

Gregg, S.J. and Sing, K.S.W. (1967) *Adsorption, Surface Area and Porosity*. Academic Press, London and New York.

Hall, P.L. and Astill, D.M. (1989) Adsorption of water by homoionic exchange forms of Wyoming bentonite (Swy-1). *Clays and Clay Minerals*, **37**, 355–363.

Harris, L.B. (1968) Adsorption on a patchwise heterogeneous surface. I. Mathematical analysis of the step-function approximation of the local isotherm. *Surface Science*, **10**, 129–145.

Harris, L.B. (1969) Adsorption on a patchwise heterogeneous surface. III. Errors incurred in using the condensation approximation to estimate the energy distribution on a Hill-De Boer adsorbent. *Surface Science*, **15**, 182–187.

Huang, W.L. (1993) The formation of illitic clays from kaolinite in KOH solution from 225 to 350°C. *Clays and Clay Minerals*, **41**, 645–654.

Jackson, M.L. and Sherman, G.D. (1952) Chemical weathering of clay minerals in soils. *Advances in Agronomy*, **5**, 219–318.

Jaroniec, M. and Brauer, P. (1986) Recent progress in determination of energetic heterogeneity of solids from adsorption data. *Surface Science Reports*, **6**, 65–117.

Jaroniec, M., Rudzinski, W., Sokolowski, S. and Smarzewski, R. (1975) Determination of energy distribution function from observed adsorption isotherms. *Journal of Colloid and Polymer Science*, **253**, 164–166.

Jozefaciuk, G. and Shin, J.S. (1996) Water vapor adsorption on soils: II. Estimation of adsorption energy distributions using local BET and Aranovich isotherms. *Korean Journal of Soil Science and Fertilizer*, **29**, 218–225.

Jozefaciuk, G., Sokolowska, Z., Sokolowski, S., Alekseev, A. and Alekseeva, T. (1993) Changes of mineralogical and surface properties of water dispersible clay after acid treatment of soils. *Clay Minerals*, **28**, 145–148.

Jozefaciuk, G., Hoffmann, C., Renger, M. and Marschner, B. (2000) Effect of extreme acid and alkali treatment on surface properties of soils. *Journal of Plant Nutrition and Soil Science*, **163**, 595–601.

Keenan, A.G., Mooney, R.W. and Wood, L.A. (1951) The relation between exchangeable ions and water adsorption on kaolinite. *Journal of Physical Colloid Chemistry*, **55**, 1462–1474.

Komadel, P., Schmidt, D., Madejová, J. and Čičel B. (1990) Alteration of smectites by treatments with hydrochloric acid and sodium carbonate solutions. *Applied Clay Science*, **5**, 113–122.

Kooyman, P.J., van der Waal, P. and Van Bekkum, H. (1997) Acid dealumination of ZSM-5. *Zeolites*, **18**, 50–53.

Kunze, G.W. (1965) Pretreatment for mineralogical analysis. Pp. 568–577 in: *Soil Analysis. Part I* (C.A. Black, editor). American Society of Agronomy, Madison, Wisconsin,.

Low, P.F. (1961) Physical chemistry of clay-water interaction. *Advances in Agronomy*, **40**, 269–327.

Madejová, J., Bujdak, J., Janek, M. and Komadel, P. (1998) Comparative FT-IR study of structural modifications during

acid treatment of dioctahedral smectites and hectorite. *Spectrochimica Acta A. Molecular and Biomolecular Spectroscopy*, **54**, 1397–1406.

Moise, J.C., Bellat, J.P. and Methivier, A. (2001) Adsorption of water vapor on X and Y zeolites exchanged with barium. *Microporous and Mesoporous Materials*, **43**, 91–101.

Myriam, M. (1998) Structural and textural modifications of palygorskite and sepiolite under acid treatment. *Clays and Clay Minerals*, **46**, 225–231.

Newman, A.C.D. (1985) The interaction of water with clay mineral surfaces. Pp. 237–274 in: *Chemistry of Clays and Clay Minerals* (A.C.D. Newman, editor). Mineralogical Society Monograph **6**. Longman Scientific and Technical, Harlow, Essex, UK.

Notario, J.S., Garcia, J.E., Caceres, J.M., Arteaga, I.J. and Gonzalez, M.M. (1995) Characterization of natural phillipsite modified with orthophosphoric acid. *Applied Clay Science*, **10**, 209–217.

Petersen, L.W., Moldrup, P., Jacobsen, O.H. and Rolston, D.E. (1996) Relations between specific surface area and soil physical and chemical properties. *Soil Science*, **161**, 9–22.

Rassineux, F., Griffault, L., Meunier, A., Berger, G., Petit, S., Vieillard, P., Zellagui, R. and Munoz, M. (2001) Expandability-layer stacking relationship during experimental alteration of a Wyoming bentonite in pH 13.5 solutions at 35 and 60ºC. *Clay Minerals*, **36**,197–210.

Ravichandran, J. and Sivasankar, B. (1997) Properties and catalytic activity of acid-modified montmorillonite and vermiculite. *Clays and Clay Minerals*, **45**, 854–857.

Ruiz, R., Blanco, C., Pesquera, C., González, F., Benito, I. and Lσpez, J.L. (1997) Zeolitization of a bentonite and its application to the removal of ammonium ion from waste water. *Applied Clay Science*, **12**, 73–83.

Rudzinski, W. and Everett, D.H. (1991) *Adsorption of Gases on Heterogeneous Surfaces*. Academic Press, London.

Rudzinski, W., Jagiello, J. and Grillet, Y. (1982) Physical adsorption of gases on heterogeneous solid surfaces: evaluation of the adsorption energy distribution from adsorption isotherms and heats of adsorption. *Journal of Colloid and Interface Science*, **87**, 478–491.

Rupert, J.P., Granquist, W.T. and Pinnavaia, T.J. (1987) Catalytic properties of clay minerals. Pp. 237–274 in: *Chemistry of Clays and Clay Minerals* (A.C.D. Newman, editor). Mineralogical Society Monograph **6**, Longman Scientific and Technical, Harlow, Essex.

Sano, T., Uno, Y., Wang, Z.B., Ahn, C.H. and Soga, K. (1999) Realumination of dealuminated HZSM-5 zeolites by acid treatment and their catalytic properties. *Microporous and Mesoporous Materials*, **31**, 89–95.

Schall, N. and Simmler-Hubenthal, H. (1995) Surface modifications of montmorillonite and resulting possibilities for use as an adsorbent. Pp. 24–25 in: *Clay and Clay Material Sciences, Proceedings of Euroclay'95, Leuven* (A. Elsen, P. Grobet, M. Keung, H. Lehman, R. Schoonheydt and H. Toufar, editors).

Shin-Jyung Kang and Kazuhiko Egashira. (1997) Modification of different grades of Korean natural zeolites for increasing cation exchange capacity. *Applied Clay Science*, **12**, 131–144.

Srasra, E. and Trabelsi-Ayedi, M. (2000) Textural properties of acid activated glauconite. *Applied Clay Science*, **17**, 71–84.

Suárez Barrios, M., Flores González, L.V., Vicente Rodríguez, M.A. and Martín Pozas, J.M. (1995) Acid activation of a palygorskite with HCl: Development of physico-chemical, textural and surface properties. *Applied Clay Science*, **10**, 247–258.

Suárez Barrios, M., de Santiago Buey, C., Garcia Romero, E. and Martin Pozas, J.M. (2001) Textural and structural modifications of saponite from Cerro del Aguila by acid treatment. *Clay Minerals*, **36**, 483–488

Šucha, V., Środoń, J., Clauer, N., Elsass, F., Eberl, D.D., Kraus, I. and Madejová, J. (2001) Weathering of smectite and illite-smectite under temperate climatic conditions. *Clay Minerals*, **36**, 403–419.

Suraj, G., Iyer, C.S.P. and Lalithambika, M. (1998) Adsorption of cadmium and copper by modified kaolinites. *Applied Clay Science*, **13**, 293–306.

Tanji, K.N. (1995) *Agricultural Salinity Assessment and Management*. Scientific Publishers, Jodphur, India.

Taubald, H., Bauer, A., Schäfer, T., Geckeis, H., Satir, M. and Kim, J.I. (2000) Experimental investigation of the effect of high-pH solutions on the Opalinus Shale and the Hammerschmiede Smectite. *Clay Minerals,* **35**, 515–524.

Thomas, G.W. and Hargrove, W.L. (1984) The chemistry of soil acidity. Pp. 3–56 in: *Soil Acidity and Liming,* 2nd edition (F. Adams, editor). American Society of Agronomy, Madison, Wisconsin.

Thorez, G. (1976) *Practical Identification of Clay Minerals*. *A Handbook*. (G. Lelotte, editor). Liege State University, Belgium.

Tombacz, E., Szerkes, M., Baranyi, L. and Micheli, E. (1998) Surface modifications of clay minerals by organic polyions. *Colloids and Surfaces A: Physical and Engineering Aspects*, **141**, 379–384.

Ulrich, B. (1990) An Ecosystem Approach to Soil Acidification. Pp. 28–79 in: *Soil Acidity*. (B. Ulrich and M.E. Sumner, editors). Springer-Verlag, Berlin.

Van Olphen, H. (1977) *An Introduction to Clay Colloid Chemistry*, 2nd edition. John Wiley & Sons, New York, London, Sydney, Toronto.

Volzone, C., Thompson, J.G., Melnitchenko, A., Ortiga, J. and Palethorpe, S.R. (1999) Selective gas adsorption by amorphous clay-mineral derivatives. *Clays and Clay Minerals*, **5**, 647–657.

Wallace, A. (1994) Soil acidification from use of too much fertilizers. *Communications in Soil Science and Plant Analysis*, **25**, 87–92.

Yatsu, E. (1988) *The Nature of Weathering. An Introduction*. Sozosha, Tokyo.

Ylagan, R.F., Altaner, S.P. and Pozzuoli A. (2000) Reaction mechanisms of smectite illitization associated with hydrothermal alteration from Ponza Island, Italy. *Clays and Clay Minerals*, **48**, 610–631.

(*Received 1 June 2001; revised 12 June 2002; Ms. 551; A.E. Peter Komadel*)